

High-power terahertz radiation emitter with a diamond photoconductive switch array

Hitoki Yoneda, Kazutatsu Tokuyama, Ken-ichi Ueda, Hironori Yamamoto, and Kazuhiro Baba

A photoconductive switch-arrayed antenna with a chemical vapor-deposited diamond film was developed to generate high-power terahertz (THz) radiation. With this device, an electric field stress of 2×10^6 V/cm can be applied to photoconductive gaps because of the high breakdown threshold of diamond and the overcoated gap structure for the prevention of surface flashover. This level of field stress can alleviate the current problem of saturation in THz emission by use of a photoconductive antenna. The device consists of more than two thousand $20 \mu\text{m} \times 2.8 \text{mm}$ emitters. In an experiment using an ultrashort pulse Kr⁺F laser, we obtained an energy density of $10 \mu\text{J}/\text{cm}^2$ on the emitter surface at $E = 10^5$ V/cm. This density was larger than that of the current large-aperture antenna. There was no severe saturation in photoconductive current up to $E = 10^6$ V/cm, and a focused intensity of $200 \text{MW}/\text{cm}^2$ can be expected. © 2001 Optical Society of America

OCIS codes: 320.7160, 320.7080, 230.0250, 320.2250, 230.6080, 320.7130.

1. Introduction

The research field that relates to ultrafast terahertz (THz) pulses has grown rapidly in recent years. The methods of generating THz pulses with an ultrashort-pulse laser can be categorized as either rectification sources^{1,2} or transit current sources.³ Among them a photoconductive (PCD) semiconductor antenna can generate intense THz waves. With this antenna there were several successful results such as real-time imaging⁴ and coherent control of Rydberg atoms.^{5,6} To date, a large-aperture antenna generates 1.7-MW, 0.8- μJ THz radiation from a 2-in. (5-cm)-diameter GaAs wafer.⁷ However, the device has several saturation problems such as shielding the applied electric field with THz radiation,⁸ carrier screening,⁸ and other mechanisms related to the saturation of PCD current.⁹ From the boundary condi-

tion, the near-field electric field of THz radiation is given by

$$E_{\text{THz}} = -E_b \frac{\sigma_s \eta_0}{\sigma_s \eta_0 + (1 + \sqrt{\epsilon_r})}, \quad (1)$$

where E_b is the applied electric field, η_0 is the free-space impedance, ϵ_r is the relative dielectric constant of the semiconductor, and σ_s is the surface photoconductivity. Equation (1) shows that, if the PCD antenna were irradiated with sufficiently intense laser light (i.e., $\sigma_s \eta_0 \sim 1$), the emitted radiation would saturate at $E_{\text{THz}} \approx E_b / (1 + \sqrt{\epsilon_r})$. Of the several limitation mechanisms, this is known to be the most severe problem for generating high-power THz radiation. For example, in an earlier version of a GaAs large-aperture antenna,⁷ the applied electric field was 10^4 V/cm, giving an estimated saturation intensity of $\sim 10^5$ W/cm². Given the effective emission area (~ 10 cm²) and pulse duration (1 ps), the saturated energy and energy density were 1 μJ and 0.1 $\mu\text{J}/\text{cm}^2$, respectively. These values are in reasonable agreement with the experimental results.⁷ Therefore, the application of a higher electric field on the PCD gap with materials having a higher breakdown strength is the only way to generate higher-power THz radiation. For this purpose, a diamond is one of the best candidates because it has the highest breakdown threshold of the various ultrafast PCD materials. In addition, recent chemical vapor-

H. Yoneda (yoneda@ils.uec.ac.jp), K. Tokuyama, and K. Ueda are with the Institute for Laser Science, University of Electrocommunications, Chofugaoka, Chofushi, Tokyo 182-8585, Japan. H. Yamamoto and K. Baba are with the Device Materials Research Laboratory, Functional Materials Research Laboratories, NEC Corporation, 4-1-1 Miyazaki, Miyamae-ku, Kawasaki, Kanagawa 216-8555, Japan.

Received 20 February 2001; revised manuscript received 3 August 2001.

0003-6935/01/366733-04\$15.00/0

© 2001 Optical Society of America

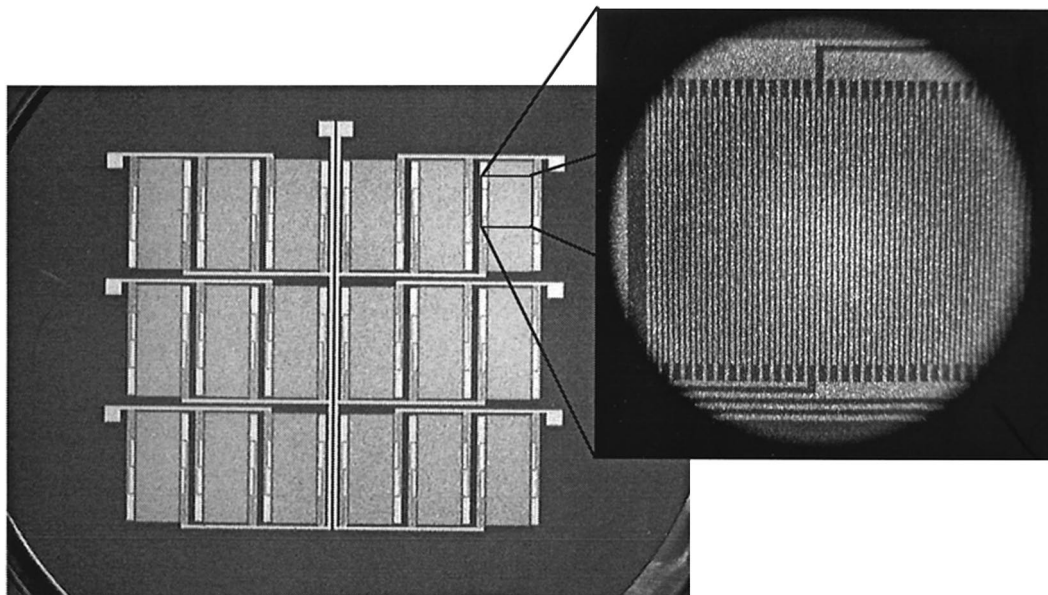


Fig. 1. Photograph of the CVD diamond THz emitter. A single unit PCD gap had a width of $20\ \mu\text{m}$ and a length of $2.8\ \text{mm}$. The total number of PCD gaps in the $3\ \text{cm} \times 3\ \text{cm}$ area was more than two thousand. To prevent degradation of the emitter performance because of a breakdown in the minor PCD gap, the gaps were divided into 18 clusters (3×6 in this figure) and were connected to a high-voltage power supply with relatively high impedance lines. The binary mask was used for amplitude spatial modulation of the illuminating laser.

deposited (CVD) growth technology has made it possible to make large-dimensional film with three-dimensional device structures.

To date, a 2-kV dc voltage can be applied to the $10\text{-}\mu\text{m}$ PCD gap with an overcoated layer to keep sufficiently high dark-current resistivity ($10^{10}\ \Omega\text{cm}$).¹⁰ This electric field strength is 2 orders of magnitude larger than that of the above-mentioned GaAs antenna. Currently, only polycrystalline crystal films can be produced with large dimensions. Typical mobilities of polycrystalline crystal are $1\text{--}70\ \text{cm}^2/\text{Vs}$,¹¹ whereas that of single diamond crystal is $1800\ \text{cm}^2/\text{Vs}$ and that of low-temperature growth GaAs is approximately $2000\text{--}3000\ \text{cm}^2/\text{Vs}$.¹² Despite the above-mentioned advantages of CVD diamond, its smaller mobility has made researchers hesitate to use it in actual device applications. However, for THz radiation applications, the effect of lower mobility in CVD diamond can be neglected because the applied electric field strength is so high that the drift velocity can reach the saturated value. For example, at $E = 1 \times 10^6\ \text{V/cm}$, the drift velocity reaches a saturated level in samples having a mobility greater than $25\ \text{cm}^2/\text{Vs}$. According to the experimental scaling law for diamond grain size dependence,¹¹ this level of mobility can be achieved in diamond film having an average grain size that is greater than $5\ \mu\text{m}$.

A photograph of our diamond PCD antenna is shown in Fig. 1. To increase the area of the PCD gap to which a high electric field strength was applied, we chose a segmented electrode design instead of a large single PCD gap geometry. We made this decision because a centimeter-sized single PCD gap with a $2 \times$

10^6-V/cm electric field strength is not a realistic design, and the ratio of leakage of the electric field outside the PCD material increased when the PCD gap width increased, causing a breakdown in the air on the boundary surface of the PCD material. In addition, if there are leakage problems in the minor single unit of the PCD gap, the effect of the defect is minor because each PCD gap is connected by relatively high-impedance feed lines. A single-unit PCD gap had a width of $20\ \mu\text{m}$ and a length of $2.8\ \text{mm}$. The number of PCD gaps was greater than two thousand and covered a $3\ \text{cm} \times 3\ \text{cm}$ area. The thickness of the overcoated layer was chosen so as to decrease the surface leakage electrical field to less than the breakdown threshold in air. There were a pair of electric field lines with opposite directions and equal electrical field strength from a single electrode. If the light spot illuminated both gaps uniformly, the electric fields that were generated would cancel each other at far-field points. To prevent this, we used a binary mask for laser light to create modulation with a large spatial wavelength. In the small emitter area, the laser illuminated the alternate elements of PCD arrays.

The width of the electrode ($40\ \mu\text{m}$) was relatively large because we wanted to prevent the electrode from snapping during the etching process (because of the surface roughness of the unpolished surface). In addition, with binary amplitude modulation of the switching laser, the ratio of the effective emission area to the whole surface area was $1/6$ [$=20\ \mu\text{m}/(20 + 40 + 20 + 40\ \mu\text{m})$]. This ratio would increase if we were to use a smaller wide electrode and a phase

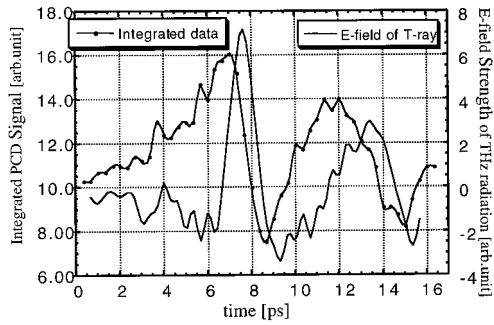


Fig. 2. Measured THz signal waveform from a CVD diamond PCD signal. Because of the longer lifetime of the PCD detector, we used the temporal derivation of the measured signal to obtain the waveform of the electric field of the THz radiation. This deconvolution is also shown. The pulse duration of the main component was 1.5 ps.

modulation method for spatial modulation of the laser pulse.

Part of this antenna (three of the 18 clusters in Fig. 1, and an effective emission PCD area of $\sim 10 \text{ mm}^2$) was irradiated with ultrashort-pulse Kr^{*}F laser light. To prevent carrier-carrier scattering, we used a laser having a photon energy of 5 eV, which is lower than the bandgap energy of 5.47 eV for diamond. The wavelength, typical output energy, and pulse width were 248 nm, 10 mJ, and 0.5 ps, respectively. Because of amplitude modulation and the mismatched shape between the emitter and the laser beam, we used approximately 1-mJ energy for generation of THz radiation. The absorption length of the CVD diamond was approximately 10 μm at this wavelength. The generated THz radiation energy was measured with a Moletron J3-05 pyroelectric detector, and the waveform and the THz focused intensity profile were measured by another diamond PCD antenna (10 $\mu\text{m} \times 2.8 \text{ mm}$) gated with an UV optical pulse. A typical waveform is shown in Fig. 2. Because the CVD diamond PCD antenna that we used had a longer carrier lifetime of 60–80 ps,¹⁴ the measured waveform was a temporal integral of the electric field of the detected THz radiation. The actual waveform of the THz electric field was estimated with a simple temporal derivation procedure under the assumption that the PCD antenna had a step-function-like response. This estimated waveform is also shown in Fig. 2. The pulse duration of the main component was 1.5 ps. The frequency spectrum of this THz radiation was calculated from a Fourier transform of the measured signal. The central frequency of this radiation was approximately 0.5 THz, and the spectrum spread from 0.1 to 2 THz.

Dependence of the THz energy on the electric field applied to the PCD antenna is shown in Fig. 3. The THz intensity was proportional to the square of the applied electric field. The emitted energy density on the THz antenna was $0.1 \mu\text{J}/\text{cm}^2$ at $E = 10^5 \text{ V}/\text{cm}$. This value exceeds that of a GaAs large-aperture antenna ($0.07 \mu\text{J}/\text{cm}^2$ at $E = 10^4 \text{ V}/\text{cm}$) even though

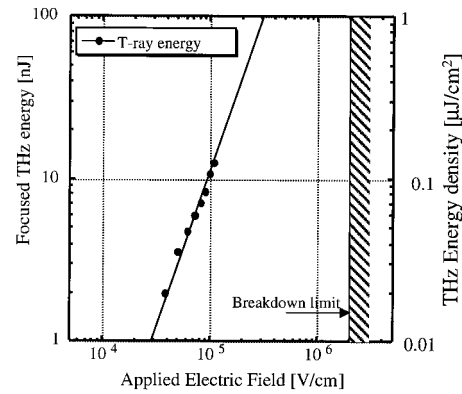


Fig. 3. Dependence of THz energy on the applied electric field at the PCD signal. The energy was proportional to the square of the applied electric field. The estimated THz energy density of the emitter surface was $0.1 \mu\text{J}/\text{cm}^2$, a value that is larger than that of the previous GaAs large-aperture antenna.

the electric field was 1/10 of the designed value of our antenna. Equation (1) with our experimental condition of $E = 10^5 \text{ V}/\text{cm}$ gives a saturated energy density of $15 \mu\text{J}/\text{cm}^2$. Therefore, this experimental condition was far from the limitation of the most severe saturation, and the energy density increases when the laser intensity increases. The PCD properties at higher electrical field strength were investigated with a single PCD switch of CVD diamond. Figure 4 shows the applied electric field dependence on the peak output voltage of the PCD signal measured with a 20-GHz sampling oscilloscope. Although there was some weak saturation in photocurrent because of the drift velocity saturation at $E > 5 \times 10^5 \text{ V}/\text{cm}$, the current increased to an approximately six times larger value at $E = 10^6 \text{ V}/\text{cm}$. These results show that the energy density of THz radiation on the emitter surface will increase by as much as 2 orders of magnitude than its present value.

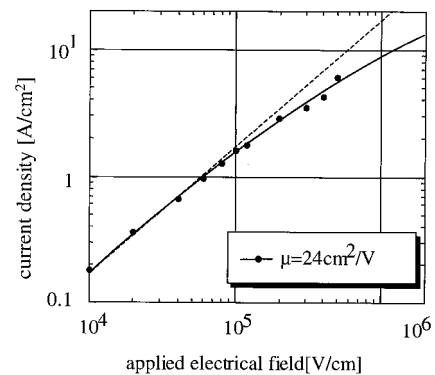


Fig. 4. Dependence of the photoconductive current on the applied electric field. Although there was a weak saturation at $E > 5 \times 10^5 \text{ V}/\text{cm}$, the photoconductive current increased by as much as six times from $1 \times 10^5 \text{ V}/\text{cm}$ to $1 \times 10^6 \text{ V}/\text{cm}$. In addition, given the estimated saturation energy density of our $3 \text{ cm} \times 3 \text{ cm}$ CVD diamond antenna, we could obtain a focusing intensity of greater than $200 \text{ MW}/\text{cm}^2$.

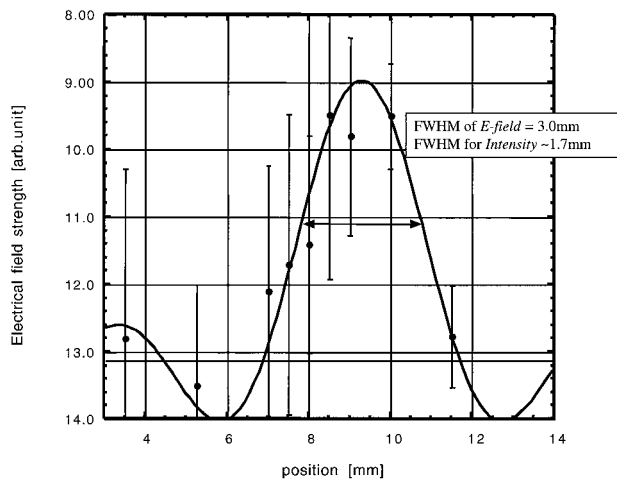


Fig. 5. Focusing profile of THz radiation with $F/2$ optics. The spot size of THz radiation was approximately $1.7 \text{ mm}\phi$. This focusability indicated the coherent addition of every element in the array antenna. The solid curve was a fitting curve with the assumption of a rectangular aperture.

The intensity profile of focused THz radiation with an $f = 15\text{-cm}$ off-axis mirror is shown in Fig. 5. The minimum spot size intensity was $1.7 \text{ mm}\phi$ FWHM, which is a reasonable value if we take into consideration the average wavelength of the THz radiation and the F -number of the focusing optics. This result reflects the coherent addition of each element. The estimated focusing power for our experiment was $3 \times 10^5 \text{ W/cm}^2$.

In conclusion, we developed a high-power THz radiation antenna with a CVD diamond PCD antenna. An electric field of $1 \times 10^6 \text{ V/cm}$ made it possible to obtain higher energy density emission. In an experiment with ultrashort-pulse Kr^*F laser light, we achieved an emission density of $0.1 \mu\text{J/cm}^2$ at $1 \times 10^5 \text{ V/cm}$. To prevent cancellation of opposite electric field components and the coherent addition of radiation from each element, we used spatial modulation with a binary mask for the laser illumination. The minimum size of $1.7 \text{ mm}\phi$ indicates that coherent addition was achieved. From PCD current experiments done at higher electric fields, the maximum electric field design ($1 \times 10^6 \text{ V/cm}$) should yield as much as a six times increase in current. In addition, we believe that an increase in laser irradiation inten-

sity and emission area will result in a focused intensity of several hundred megawatts per square centimeter from a 2-in. (5-cm)-diameter wafer-sized emitter in the near future.

References

1. K. P. Yang, P. L. Richards, and Y. R. Shen, "Generation of far-infrared radiation by picosecond light pulses in LiNbO_3 ," *Appl. Phys. Lett.* **19**, 320–323 (1971).
2. Y. R. Shen, "Far-infrared generation by optical mixing," *Prog. Quantum Electron.* **4**, 207–238 (1976).
3. D. H. Auston, K. P. Cheung, and P. R. Smith, "Picosecond photoconducting Hertzian dipoles," *Appl. Phys. Lett.* **45**, 284–286 (1984).
4. Z. Jiang and X.-C. Zhang, "Electro-optics measurement of THz field pulses with a chirped optical beam," *Appl. Phys. Lett.* **72**, 1945–1947 (1998).
5. R. R. Jones, D. You, and P. H. Bucksbaum, "Ionization of Rydberg atoms by subpicosecond half-cycle electromagnetic pulses," *Phys. Rev. Lett.* **70**, 1236–1239 (1993).
6. J. Ahn, D. N. Hutchinson, C. Rangan, and P. H. Bucksbaum, "Quantum phase retrieval of a Rydberg wave packet using a half-cycle pulse," *Phys. Rev. Lett.* **86**, 1179–1182 (2001).
7. D. You, R. R. Jones, P. H. Bucksbaum, and D. R. Dykaar, "Generation of high-power sub-single-cycle 500-fs electromagnetic pulses," *Opt. Lett.* **18**, 290–292 (1993).
8. B. B. Hu, J. T. Darrow, X.-C. Zhang, D. H. Auston, and P. R. Smith, "Optically steerable photoconductive antennas," *Appl. Phys. Lett.* **56**, 886–888 (1990).
9. G. Rodriguez and A. J. Taylor, "Screening of the bias field in terahertz generation from photoconductors," *Opt. Lett.* **21**, 1046–1048 (1996).
10. G. Rodriguez, S. R. Caceres, and A. J. Taylor, "Modeling of terahertz radiation from biased photoconductors: transient velocity effects," *Opt. Lett.* **19**, 1994–1996 (1994).
11. H. Yoneda, K. Ueda, Y. Aikawa, K. Baba, and N. Shohata, "Photoconductive properties of chemical vapor deposited diamond switch under high electric field strength," *Appl. Phys. Lett.* **66**, 460–462 (1995).
12. H. Yoneda, K. Ueda, Y. Aikawa, K. Baba, and N. Shohata, "The grain size dependence of the mobility and lifetime in chemical vapor deposited diamond photoconductive switches," *J. Appl. Phys.* **83**, 1730–1733 (1998).
13. H. Nemeč, A. Pashkin, P. Kuzel, M. Khazan, S. Schnell, and I. Wilke, "Carrier dynamics in low-temperature grown GaAs studied by terahertz emission spectroscopy," *J. Appl. Phys.* **90**, 1303–1306 (2001).
14. H. Yoneda, K. Tokuyama, R. Yamazaki, K. Ueda, H. Yamamoto, and K. Baba, "Effect of grain boundaries on carrier lifetime in chemical-vapor-deposited diamond film," *Appl. Phys. Lett.* **77**, 1425–1428 (2000).